Molecular Neurobiology (2019) 56:907–919
https://doi.org/10.1007/s12035-018-1119-4

Infantile Amnesia Is Related to Developmental Immaturity of the Maintenance Mechanisms for Long-Term Potentiation

Tsung-Chih Tsai[1] · Chiung-Chun Huang[2] · Kuei-Sen Hsu[1,2]

Received: 16 January 2018 / Accepted: 11 May 2018 / Published online: 26 May 2018
© Springer Science+Business Media, LLC, part of Springer Nature 2018

Abstract

Infantile amnesia (IA) refers to the inability of adults to recall episodic memories from infancy or early childhood. While several hypotheses have been proposed to explain the occurrence of IA, the neurobiological and molecular bases for this accelerated forgetting phenomenon remain elusive. Using hippocampus-dependent object-location memory and contextual fear conditioning tasks, we confirmed that infant mice trained at postnatal day 20 (P20) displayed deficits in long-term memory retention compared to adult (P60) mice. The percentage of CA1 pyramidal neurons expressing phosphorylated cAMP-responsive element-binding protein after fear conditioning was significantly lower in P20 than P60 mice. P20 mice exhibited attenuated basal excitatory synaptic transmission and early-phase long-term potentiation (E-LTP) at Schaffer collateral-CA1 synapses compared to P60 mice, but conversely, P20 mice have a greater susceptibility to induce time-dependent reversal of LTP by low-frequency afferent stimulation than P60 mice. The protein levels of GluN2B subunit of *N*-methyl-D-aspartate receptors (NMDARs), protein kinase Mζ (PKMζ), and protein phosphatase 2B (PP2B) in hippocampal CA1 region were significantly higher in P20 than P60 mice. We also found that the levels of calcium/calmodulin-dependent protein kinase II α autophosphorylation at Thr286, GluA1 phosphorylation at Ser831, and PKMζ protein biosynthesis occurred during the ensuing maintenance of E-LTP were significantly lower in P20 than P60 mice. Pharmacological blockade of GluN2B-containing NMDARs or PP2B effectively restored deficits of E-LTP and long-term memory retention observed in P20 mice. Altogether, these findings suggest that developmental immaturity of the maintenance mechanisms for E-LTP is linked to the occurrence of IA.

Keywords Infantile amnesia · Long-term potentiation · *N*-methyl-D-aspartate receptor · Protein phosphatase 2B · Hippocampus

Introduction

Adults rarely remember events that occurred during infancy or early childhood, a phenomenon called "infantile amnesia (IA)" or "childhood amnesia" [1]. While IA was initially described in humans, it was subsequently identified as a ubiquitous phenomenon that occurs in all altricial species, making it an excellent model for translational research on "normal forgetting" [2, 3]. Although the underlying causes of IA are not certain, several hypotheses have been proposed to explain its occurrence. For example, the information processing hypothesis postulates that IA may result from failures at memory encoding, storage, and/or retrieval [4]. In support of this hypothesis, experiments in both humans and rodents have revealed that reminder treatment is able to reinstate memories acquired during early life, suggesting that IA is due to a retrieval failure [5–8]. However, it has yet to be determined whether IA is always retrieval failure or may in part be caused by acquisition, consolidation, or storage failure. In addition, the current neurogenic hypothesis postulates that IA is related to high levels of neurogenesis in the infant brain [4, 9]. Support for this hypothesis comes from the findings that reducing neurogenesis in the hippocampus can mitigate forgetting in infant mice [10]. However, neurogenic hypothesis fails to explain why hippocampus-independent memories acquired during the IA period are also forgotten at an accelerated rate [1].

Over the past two decades, there have been tremendous efforts to explore the cellular and molecular mechanisms underpinning the acquisition and storage of long-term memory in the adult brain [11, 12]; however, little is known about the neurobiological mechanisms underlying the formation of infantile

✉ Kuei-Sen Hsu
richard@mail.ncku.edu.tw

[1] Institute of Basic Medical Sciences, College of Medicine, National Cheng Kung University, Tainan 701, Taiwan

[2] Department of Pharmacology, College of Medicine, National Cheng Kung University, No. 1, University Rd, Tainan 701, Taiwan

memories. Based on the information processing hypothesis, it is possible that IA occurs because key molecular mechanisms for memory acquisition and storage are insufficiently mature during the IA period. As long-term potentiation (LTP) is a leading cellular basis of long-term memory [13] and there is now compelling evidence that LTP and memory are supported by similar molecular mechanisms [14, 15], LTP may provide both practical and theoretical advantages for elucidating the mechanisms that drive accelerated forgetting during infancy. Conceptually, LTP involves the preferential activation of protein kinases, and protein phosphatases have key role in limiting LTP induction and maintenance [16, 17]. Because the protein kinase activity required for LTP changes during early postnatal development [18, 19], we undertook this study to examine whether developmental immaturity of the maintenance mechanisms for LTP could contribute the occurrence of IA. Specifically, we hypothesize that IA is driven by an imbalance in the expression of protein kinases and phosphatases, which have opposite effects on memory acquisition and maintenance during both later in life and early in development. Our results demonstrate that excess GluN2B subunit of *N*-methyl-D-aspartate receptor (NMDAR) activation and protein phosphatase 2B (PP2B) activity in hippocampal CA1 region early in life promote LTP decay lead to impaired memory maintenance and ultimately result in IA.

Materials and Methods

Animals

Twenty- and sixty-day-old male C57BL/6 mice were used in all experiments. Mice were housed in groups of four in a temperature (25 ± 1 °C) and humidity controlled room on a 12-h light-dark cycle with food and water provided ad libitum. All behavioral procedures were carried out during the light cycle between 7:00 and 10:00 h. All experimental procedures complied with the National Institutes of Health Guide for the Care and Use of Laboratory Animals and were approved by the Institutional Animal Care and Use Committee of National Cheng Kung University.

Object-Location Memory Task

Object-location memory (OLM) task was performed as previously described [20]. Before the training session, mice were habituated to the experimental apparatus (40 × 40 × 40 cm^3) by allowing them to freely explore for 10 min for 1 day in the absence of objects. During the training session, two identical objects were presented for exploration for 10 min. During the testing session, 1 or 24 h later, object exploration was scored for 10 min. Locomotor activity and the time spent in exploring each object were recorded using a digital video camera, and scoring was performed with the behavioral tracking system Ethovision (Noldus). Object exploration was defined as the mouse's head being oriented toward the object within a distance of 2 cm or the mouse's nose touching the object. To analyze cognitive performance, a discrimination index was calculated as the following formula: [(time exploring the object in novel location − time exploring the object in familiar location) / (time exploring the objects in both novel and familiar locations)].

Contextual Fear Conditioning

The contextual fear conditioning (CFC) test was conducted using a computer-controlled context conditioning system (ENV-307A, MED Associates) as previously described [10]. Mice were placed into the conditioning chamber (15.9 × 14.0 × 12.7 cm) and allowed to explore the same context for 2 min followed by one or three aversive electrical footshocks (2 s, 0.60 mA with 30 s intershock interval) through a stainless steel grid floor. After the last shock, mice were allowed to explore the context for additional 2 min prior to return to their home cages. The behavior of the mice was recorded using a digital near-infrared video camera on the ceiling of the sound attenuating cubicle. Context-dependent freezing responses were measured 1 or 24 h after fear conditioning training. The freezing responses were scored as the total time spent freezing in the conditioning context during the 3 min test session.

Slice Preparations and Electrophysiology

Hippocampal slices were prepared using standard procedures as previously described [20]. The mice were anesthetized with isoflurane and euthanized by decapitation. The brains were rapidly removed and placed in ice-cold sucrose artificial cerebrospinal fluid (aCSF) cutting solution [containing (in mM): sucrose 234, KCl 2.5, $CaCl_2$ 0.5, $MgCl_2$ 7, $NaHCO_3$ 25, NaH_2PO_4 1.25, and glucose 11 at pH 7.3–7.4 and equilibrated with 95% O_2–5% CO_2]. Coronal hippocampal slices (250 or 400 μm) were prepared using a vibrating microtome (VT1200S; Leica) and transferred to a holding chamber of normal aCSF [containing (in mM): NaCl 117, KCl 4.7, $CaCl_2$ 2.5, $MgCl_2$ 1.2, $NaHCO_3$ 25, NaH_2PO_4 1.2, and glucose 11 at pH 7.3–7.4 and equilibrated with 95% O_2–5% CO_2] and maintained at room temperature for at least 1 h before use.

During each electrophysiological recording session, one slice was transferred to the recording chamber and continually perfused with oxygenated aCSF at a flow rate of 2–3 ml/min at 32.0 ± 0.5 °C. The extracellular field potential recordings were carried out using an Axoclamp-2B amplifier (Molecular Devices). Microelectrodes were pulled from microfiber-filled 1.0 mm capillary tubing on a Brown-Flaming electrode puller (Sutter Instruments). The responses were low pass filtered at 2 kHz, digitally sampled at 10 kHz, and analyzed using

pCLAMP 8.0 software (Molecular Devices). Postsynaptic responses were evoked in CA1 stratum radiatum by extracellular stimulation of Schaffer collateral/commissural afferents at 0.033 Hz with a bipolar tungsten stimulating electrode. The stimulation strength was set to elicit response for which the amplitude was 30–40% of the maximum spike-free response. Field excitatory postsynaptic potentials (fEPSPs) were recorded with a glass pipette filled with 1 M NaCl (2–3 MΩ resistance), and the fEPSP slope was measured from approximately 20–70% of the rising phase using a least-squares regression. Paired pulse facilitation (PPF) was assessed by using a succession of paired pulses separated by intervals of 20, 40, 60, 80, 100, and 200 ms. The early-phase LTP (E-LTP) was induced by high-frequency stimulation (HFS), at the test pulse intensity, consisting of one or two 1 s trains of stimuli separated by an intertrain interval of 20 s at 100 Hz, and late-phase LTP (L-LTP) was induced by four 1 s trains of 100 Hz stimuli separated by an intertrain interval of 5 min. Depotentiation (DEP) was induced by application of 10 min low-frequency stimulation (LFS) at 2 Hz. The magnitudes of LTP were averaged the responses recorded during the last 10 min of the recording and normalized to 10 min of baseline before LTP induction. The magnitudes of DEP were calculated by comparing the averaged responses recorded at 50–60 min after the end of LFS with the individual baseline magnitude just before each LFS application.

Whole-cell patch-clamp recordings were made from visualized pyramidal neurons in the CA1 region of hippocampal slices using an Axopatch 200B amplifier (Molecular Devices). Data acquisition and analysis were performed using a digitizer (Digidata 1440A) and pCLAMP 9 software (Molecular Devices). For measurement of synaptically evoked excitatory postsynaptic currents (EPSCs), a bipolar stimulating electrode was placed in the stratum radiatum of CA1 region to stimulate Schaffer collateral/commissural afferents at 0.05 Hz and the superfusate routinely contained gabazine (10 μM) to block $GABA_A$ receptor-mediated inhibitory synaptic responses. EPSCs were recorded in voltage-clamp mode at a holding potential of − 70 mV. The composition of intracellular solution was as follows (mM): 130 cesium-methanesulfonate, 10 HEPES, 0.5 EGTA, 8 NaCl, 1 TEA, 4 Mg-ATP, 0.4 Na-GTP, 10 Na-phosphocreatine, and 1 QX-314. The NMDAR/α-amino-3-hydroxy-5-methyl-4-isoxazolepropionic acid receptor (AMPAR) ratio was computed by dividing the peak amplitude of the NMDAR-mediated EPSCs recorded at + 40 mV by the peak amplitude of the AMPAR-mediated EPSCs recorded at − 70 mV. The NMDAR-mediated component of EPSCs was calculated as the difference between the EPSCs measured in the absence and presence of 2-amino-5-phosphonovaleric acid (APV, 50 μM). Miniature EPSCs (mEPSCs) were recorded from CA1 pyramidal neurons held in voltage-clamp mode at a holding potential of − 70 mV in the presence of tetrodotoxin (0.5 μM) and gabazine (10 μM), and analyzed offline using a commercially available software (Mini Analysis 4.3; Synaptosoft) as previously described [21]. Detection threshold for analysis was set at twice the root-mean-square (RMS) noise levels.

Western Blotting

The microdissected hippocampal CA1 tissue samples were lysed in ice-cold Tris-HCl buffer solution (TBS; pH 7.4), containing a cocktail of protein phosphatase and proteinase inhibitors, and ground with a pellet pestle (Kontes glassware) as previously described [22]. Samples were sonicated and spun down at 14,500 rpm at 4 °C for 15 min. The supernatant was then assayed for total protein concentration using Bio-Rad Bradford Protein Assay Kit (Hercules). Each sample from tissue homogenate was separated using 8 or 10% SDS-PAGE gel. Following the transfer on polyvinylidene fluoride membranes, blots were blocked in buffer solution containing 3% bovine serum albumin (BSA) and 0.4% Tween-20 in phosphate-buffered saline (PBS) (in mM: 124 NaCl, 4 KCl, 10 Na_2HPO_4, and 10 KH_2PO_4; pH 7.2) for 1 h and then blotted overnight at 4 °C with the antibodies that recognize phosphorylated calcium/calmodulin-dependent protein kinase II α (CaMKIIα) at Thr286 (1:1000; Cat# MA1-047; Thermo Fisher Scientific), phosphorylated GluA1 at Ser831 (1:1000; Cat# 04-823; Millipore), GluN1 (1:1000; Cat# sc-1467; Santa Cruz Biotechnology), GluN2A (1:1000; Cat# sc-1468; Santa Cruz Biotechnology), GluN2B (1:1000; Cat# 14544S; Cell Signaling Technologies), PKMζ (1:1000; Cat# sc-216; Santa Cruz Biotechnology), protein phosphatase 1 (PP1; 1:1000; Santa Cruz Biotechnology; mouse; sc-7482), PP2A (1:1000; Cat# 05-421; Millipore), PP2B (1:1000; Cat# 07-069; Upstate Biotechnology), or β-actin (1:10000; Cat# MAB1501; Millipore). It was then probed with HRP-conjugated secondary antibody for 1 h and developed using the ECL Plus™ immunoblotting detection system (Amersham Biosciences), according to manufacturer's instructions. The immunoblots using phosphorylation site-specific antibodies were subsequently stripped and reprobed with the following antibodies: anti-CaMKIIα antibody (1:1000; Cat# MA1-048; Thermo Fisher Scientific) or anti-GluA1 antibody (1:1000; Cat# ab86141; Abcam). Immunoblots were analyzed by densitometry using Bio-profil BioLight PC software (Vulber Lourmat). Only film exposures that were not saturated were used for quantification analysis.

Immunofluorescence

Immunofluorescence was performed as previously described [20]. Immediately after fear conditioning, mice were deeply anesthetized through intraperitoneal injection of sodium pentobarbital (100 mg/kg) and perfused transcardially with PBS and 4% paraformaldehyde. After the perfusion, the brains

were removed and fixed in 4% paraformaldehyde for 24 h at 4 °C and then transferred to the solution containing 30% sucrose that immersed in 4 °C for at least 48 h before slicing. Coronal slices were sectioned to a 40-μm thickness, washed with 0.3% Triton X-100, and then incubated for blocking with solution containing 3% goat serum in PBS. After blocking, the sections were incubated in the primary antibodies against phosphorylated cAMP response element-binding protein at Ser133 (pCREB, 1:1000; Cat# 06-519; Millipore) or neuronal nuclei (NeuN, 1:2000; Cat# MAB377; Millipore) overnight at 4 °C in PBS with 0.1% Triton X-100. Finally, sections were washed with TBS containing 0.1% Tween-20 and then incubated with the secondary Alexa Fluor 488 or Alexa Fluor 568 antibodies (Invitrogen) for 1 h at room temperature. The immunostained sections were collected on separate gelatin-subbed glass slides, rinsed extensively in PBS, and mounted with ProLong Gold Antifade Reagent (Invitrogen). Fluorescence images of neurons were obtained using an Olympus FluoView FV1000 confocal microscope with sequential acquisition setting at a resolution of 1024 × 1024 pixels and a sampling of six consecutive optical sections in the Z-stack. The high magnification images were recorded with an Olympus Plan Apochromat × 60 oil-immersion objective (1.42 numerical aperture and 0.15 working distance). All images were imported into NIH ImageJ software (National Institutes of Health) for analysis, and all the parameters used were kept consistent during capturing.

Hippocampal Cannula Implantation and Drug Injection

On P11 and P51, mice were bilaterally implanted under deep pentobarbital (50 mg/kg, i.p. supplemented as required) anesthesia with 28-gauge guide cannulas (Plastics One Inc., Roanoke, VA) in the dorsal hippocampus. Coordinates for P11 mice were − 1.8 mm posterior to bregma, ± 1.5 mm bilateral to midline, and 1.3 mm ventral to brain surface and for P51 mice were − 2.0 mm posterior to bregma, ± 1.5 mm bilateral to midline, and 1.5 mm ventral to brain surface according to the Golgi atlas of the postnatal mouse brain [23] and the stereotaxic atlas of adult mouse brain [24]. The cannulas were fixed to the skull with dental cement. Dummy cannulas (33 gauge) were inserted into each guide cannula following the surgery to prevent clogging. Mice were allowed to recover from surgery for 1 week prior to cannula infusion and behavioral training. Cyclosporin A (0.2 μg/μl) or ifenprodil (5 μg/μl) was bilaterally administered into the hippocampus at the rate of 0.25 μl/min (0.5 μl/side) 15 min before the behavioral training by using a 33-gauge needle that connected via polyethylene tubing to a Hamilton syringe. Cyclosporin A was dissolved in 10% dimethyl sulfoxide (DMSO) in PBS. Ifenprodil was dissolved in PBS. Drug dose was selected on the basis of published studies [25, 26]. The infusion cannulas were kept in place for an additional 2 min to minimize backflow of the injectant. Histological verification of the cannula locations was performed at the end of behavioral testing. Mice with misplaced cannulas were excluded from behavioral analysis.

Statistical Analysis

The results are presented as mean ± SEM. Statistical analyses were performed using the Prism 6 software package (GraphPad Software). To compare the difference between the means of two distributions, we first determined whether the distributions of values were Gaussian using the Shapiro-Wilk test. For Gaussian distributions, we calculated p values using unpaired Student's t test, while for non-Gaussian distributions, we used Mann-Whitney U test. Because the distributions of LTP and DEP magnitudes were not Gaussian, the Mann-Whitney U test was used to compare differences between two independent groups. The significance of the difference between multiple groups was calculated by two-way analysis of variance (ANOVA) followed by Bonferroni's post hoc analyses. The number of animals used is indicated by n. Electrophysiological values across multiple slices or neurons from the same animal were averaged to yield a single value for each animal. Probability values of $p \leq 0.05$ were considered to represent significant differences.

Results

Infant and Adult Mice Show Different Memory Retentions

We first compared the ability of infant (P20) and adult (P60) mice to form enduring hippocampus-dependent memories using the OLM and CFC tasks. As shown in Fig. 1a, when mice were tested short-term OLM 1 h after training, both P20 and P60 mice had intact memory retention. They both spent more time exploring the object in the novel location than the one in the original location ($t_{(14)} = 0.20$, $p = 0.85$; unpaired Student's t test). However, when tested long-term OLM 24 h after training, P20 mice exhibited significantly reduced discrimination index compared to P60 mice ($t_{(35)} = 3.61$, $p < 0.001$; unpaired Student's t test; Fig. 1b), whereas no differences between the groups in overall exploration of objects were observed. In CFC tests, both short-term memory and long- term memory were assessed. There was no difference between P20 and P60 mice in memory retention test 1 h (short-term memory) after a single context-shock pairing fear conditioning training ($t_{(8)} = 0.85$, $p = 0.42$; unpaired Student's t test; Fig. 1c). However, P20 mice froze significantly less than P60 mice when tested 24 h postconditioning (long-term memory) ($t_{(19)} = 3.80$, $p < 0.01$; unpaired Student's t test; Fig. 1d). When mice received fear conditioning to contextual

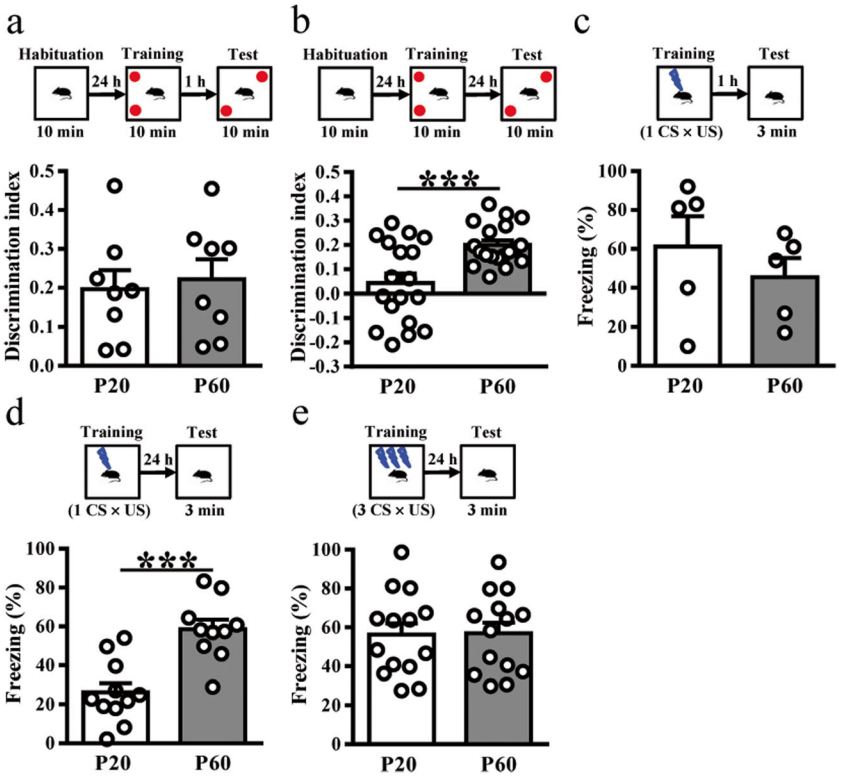

Fig. 1 Infant and adult mice show differential retention of OLM and CFC memories. **a**, **b** Schematic representations of the OLM task (upper panel). Mice were habituated to the experimental apparatus for 10 min and 24 h before OLM training session. During the training session, mice were given 10 min to explore two identical objects. For retention test, one object was placed in the familiar location and one was moved to a different location. The discrimination index was calculated as the difference in time spent exploring the novel location minus the time spent exploring the familiar location over the total exploration time during the test session. Summary bar graphs depicting the memory retention testing at 1 h (**a**) ($n = 8$ in each group) or 24 h (**b**) after training ($n = 18$ in each group). **c**, **d** Schematic representations of the training protocol for the CFC test (upper panel). Summary bar graphs depicting the fear memory retention test at 1 h (**c**) ($n = 5$ in each group) or 24 h (**d**) after receiving one conditioned stimulus (CS) × unconditioned stimulus (US) paired training (P20, $n = 11$ and P60, $n = 10$) in P20 and P60 mice. **e** Schematic representations of the training protocol for the CFC test (upper panel). Summary bar graphs depicting the fear memory retention test at 24 h after receiving three CS × US paired training ($n = 14$ in each group) in P20 and P60 mice. ***$p < 0.001$ compared with P60 group. Error bars indicate SEM

stimuli paired with three shocks, P20 and P60 mice exhibited comparable levels of freezing in the conditioning context when tested 24 h postconditioning ($t_{(22)} = 0.30$, $p = 0.77$; unpaired Student's t test; Fig. 1e). P20 and P60 mice have no differences in foot-shock pain sensitivity.

Because CREB phosphorylation (pCREB) at Ser133 correlates with memory formation [27, 28], we compared the percentages of CA1 neurons expressing pCREB immediately after a single context-shock pairing fear conditioning. We observed significantly lower percentages of CA1 neurons expressed pCREB after a single context-shock pairing fear conditioning training in both dorsal (DH) and ventral hippocampus (VH) of P20 mice compared to those in P60 mice (DH: $t_{(10)} = 2.61$, $p < 0.05$; VH: $t_{(10)} = 2.30$, $p < 0.05$; unpaired Student's t test; Fig. 2a, b). However, there was no difference between P20 and P60 mice in percentages of CA1 neurons expressed pCREB immediately after three context-shock pairing fear conditioning training in both DH ($t_{(6)} = 0.85$, $p = 0.43$; unpaired Student's t test) and VH ($t_{(6)} = 1.31$, $p = 0.24$; unpaired Student's t test; Fig. 2c, d).

Infant and Adult Mice Show Different Synaptic Transmissions and Plasticities

To investigate the potential cellular basis of IA, we compared the basal synaptic transmission and the induction of long-term synaptic plasticity at Schaffer collateral-CA1 synapses in hippocampal slices from P20 and P60 mice. Consistent with previous findings [29], we found that P20 mice exhibited smaller fEPSP slopes at different stimulus intensities compared to P60 mice. Two-way ANOVA revealed a significant age × stimulus intensity interaction ($F_{(11120)} = 2.72$, $p < 0.01$), a significant effect of age ($F_{(1,120)} = 33.09$, $p < 0.001$), and a significant effect of stimulus intensity ($F_{(11120)} = 101.7$, $p < 0.001$; Fig. 3a). To determine whether P20 and P60 mice have different presynaptic function, we examined the PPF, a transient form of presynaptic plasticity. As shown in Fig. 3b, pairs of presynaptic fiber stimulation pulses delivered over an interpulse interval range of 20–200 ms evoked higher amounts of PPF ratio in slices from P20 mice than those from P60 mice. Two-way repeated measure ANOVA revealed a significant effect of age ($F_{(1,60)} = 25.70$, $p < 0.01$) and a

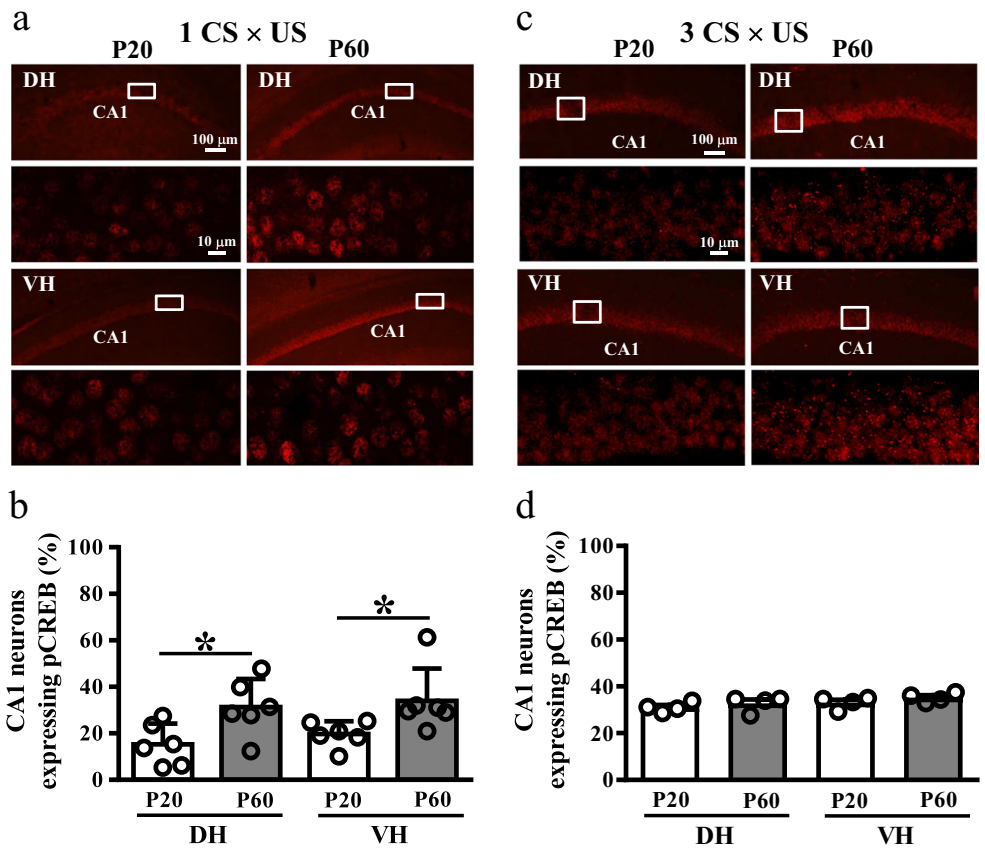

Fig. 2 The expression of pCREB in CA1 pyramidal neurons immediately after context-shock pairing fear conditioning. **a** Representative immunofluorescence images showing pCREB-expressing neurons in the dorsal (DH) or ventral (VH) hippocampal CA1 region of P20 and P60 mice immediately after fear conditioning. Augmented figures (lower panel) showing pCREB-expressing CA1 neurons in rectangle area. **b** Quantitative analysis of percentage of CA1 neurons expressing pCREB ($n = 6$ in each group). **c** Representative immunofluorescence images showing pCREB-expressing neurons in the dorsal (DH) or ventral (VH) hippocampal CA1 region of P20 and P60 mice immediately after three context-shock pairing fear conditioning training. Augmented figures (lower panel) showing pCREB-expressing CA1 neurons in rectangle area. **d** Quantitative analysis of percentage of CA1 neurons expressing pCREB ($n = 4$ in each group). *$p < 0.05$ compared with P60 group. Error bars indicate SEM

significant effect of interpulse interval ($F_{(5,60)} = 4.88, p < 0.001$), but a non-significant effect for the interaction between age and interpulse interval ($F_{(5,60)} = 0.05, p = 0.99$). However, we found no significant difference in the NMDAR/AMPAR ratio of evoked EPSCs in slices from P20 and P60 mice ($t_{(9)} = 0.33$, $p = 0.75$; unpaired Student's t test; Fig. 3c). Furthermore, the frequency ($t_{(10)} = 4.51$, $p < 0.01$; unpaired Student's t test) but not the amplitude ($t_{(10)} = 0.34$, $p = 0.74$; unpaired Student's t test) of mEPSCs was significantly lower in slices from P20 mice compared to those from P60 mice (Fig. 3d).

We next compared the magnitude of hippocampal CA1 LTP in slices from P20 and P60 mice. In slices from P60 mice, a single train of HFS (100 Hz, 1 s) induced a robust E-LTP (41.7 ± 7.0%), whereas a significantly faster decay of E-LTP was observed in slices from P20 mice (10.2 ± 5.1%, $p < 0.01$; Mann-Whitney U test; Fig. 3e, h). In contrast, we observed no significant difference between P20 and P60 mice in the induction of E-LTP by two trains of HFS ($p = 0.48$; Mann-Whitney U test; Fig. 3f, h) or L-LTP by four trains of HFS ($p = 0.68$; Mann-Whitney U test; Fig. 3g, h). To compare the ability of LFS-induced DEP in slices from P20 and P60 mice, LFS was applied 10 or 30 min after two trains of HFS. The magnitude of DEP was similar between P20 and P60 mice when LFS was applied 10 min after HFS ($p = 0.18$; Mann-Whitney U test; Fig. 3i, k). In contrast, when LFS was applied 30 min after HFS, the higher magnitude of DEP was observed in slices from P20 mice compared to those from P60 mice ($p = 0.03$; Mann-Whitney U test; Fig. 3j, k).

Infant and Adult Mice Show Different Expression Profiles of Protein Kinases and Phosphatases

We then compared the hippocampal CA1 expression profiles of molecules known to play critical roles in LTP and memory formation, either in basal condition or following LTP induction, using Western blot analyses in DH CA1 tissue extracts from P20 and P60 mice. P20 mice had a significant higher level of GluN2B protein compared to P60 mice ($t_{(10)} = 3.24$, $p < 0.01$;

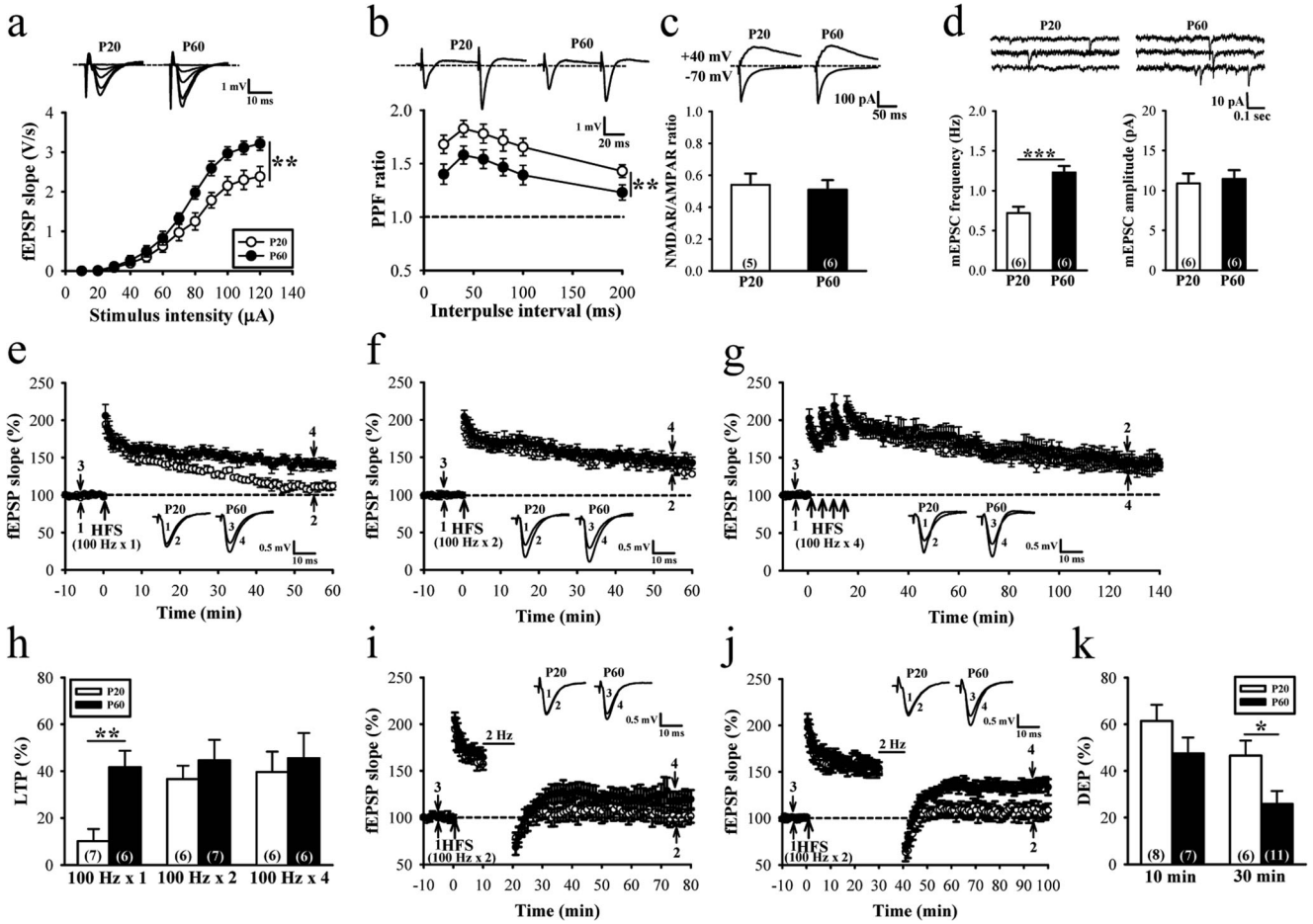

Fig. 3 P20 and P60 mice show differential excitatory synaptic transmission and long-term plasticity in hippocampal CA1 neurons. **a** Input-output curve of fEPSP (V/s) versus stimulus intensity (μA) at Schaffer collateral-CA1 synapses in slices from P20 and P60 mice. **b** Comparison of paired pulse facilitation (PPF) ratio of fEPSPs at Schaffer collateral-CA1 synapses in slices from P20 and P60 mice. **c** Representative traces and summary data comparing the NMDAR/AMPAR ratio of EPSCs in hippocampal CA1 neurons in slices from P20 and P60 mice. NMDAR/AMPAR ratio was computed by dividing the peak amplitude of the NMDAR-mediated EPSCs recorded at + 40 mV by the peak amplitude of the AMPAR-mediated EPSCs recorded at − 70 mV. **d** Representative traces showing the mEPSCs of hippocampal CA1 neurons in slices from P20 and P60 mice. Summary bar graphs showing comparisons between P20 and P60 mice in the averaged frequency (left) and amplitude (right) of mEPSCs. **e**–**g** Summary of experiments showing comparisons between P20 and P60 mice in the induction of hippocampal CA1 LTP by one (**e**), two (**f**), or four trains (**g**) of high-frequency stimulation (HFS, 100 Hz, 1 s). **h** Summary bar graphs comparing average magnitudes of LTP in slices from P20 and P60 mice. The magnitudes of LTP were measured at 50–60 min (**e**, **f**) and 110–120 min (**g**) after HFS. **i**, **j** Summary of experiments showing the induction of low-frequency stimulation (LFS, 2 Hz, 10 min)-induced depotentiation (DEP) in slices from P20 and P60 mice. LFS was applied at 10 min (**i**) or 30 min (**j**) after LTP induction. **k** Summary bar graphs comparing average magnitudes of DEP in slices from P20 and P60 mice. The magnitudes of DEP were measured at 50–60 min after the end of LFS. The total number of animal examined is indicated by *n* in parenthesis. $*p < 0.05$ and $***p < 0.001$ compared with P60 group. Error bars indicate SEM

unpaired Student's *t* test), whereas the levels of GluN1 and GluN2A proteins were not different between groups (Fig. 4a). In addition, there was a significant higher level of PKMζ ($t_{(12)} = 4.08$, $p < 0.01$; unpaired Student's *t* test; Fig. 4b) and PP2B ($t_{(12)} = 3.64$, $p < 0.01$; unpaired Student's *t* test; Fig. 4c) in P20 mice compared to P60 mice. No significant differences were found in the levels of CaMKIIα, GluA1, PP1, and PP2A between P20 and P60 mice in basal condition (Fig. 4b, c). To determine LTP-associated activation of CaMKII and GluA1 phosphorylation, slices were harvested at different time points after a single train of HFS and measured for their pCaMKIIα (Thr286) and pGluA1 (Ser831) and total CaMKIIα and GluA1 levels. In slices from P60 mice, HFS led to pronounced and significant increase in pCaMKIIα and pGluA1 levels, which continued up to 60 min after HFS. In contrast, HFS in slices from P20 mice did not significantly alter pCaMKIIα and pGluA1 levels. Two-way ANOVA followed by Bonferroni's post hoc test revealed that P20 mice had significant lower levels of pCaMKIIα ($F_{(4,70)} = 3.69$, $p < 0.01$) and pGluA1 ($F_{(4,70)} = 4.43$, $p < 0.01$) compared to P60 mice ($p < 0.01$; Fig. 4d–f). There were no differences between the groups in total CaMKIIα and GluA1 levels at any time point after HFS.

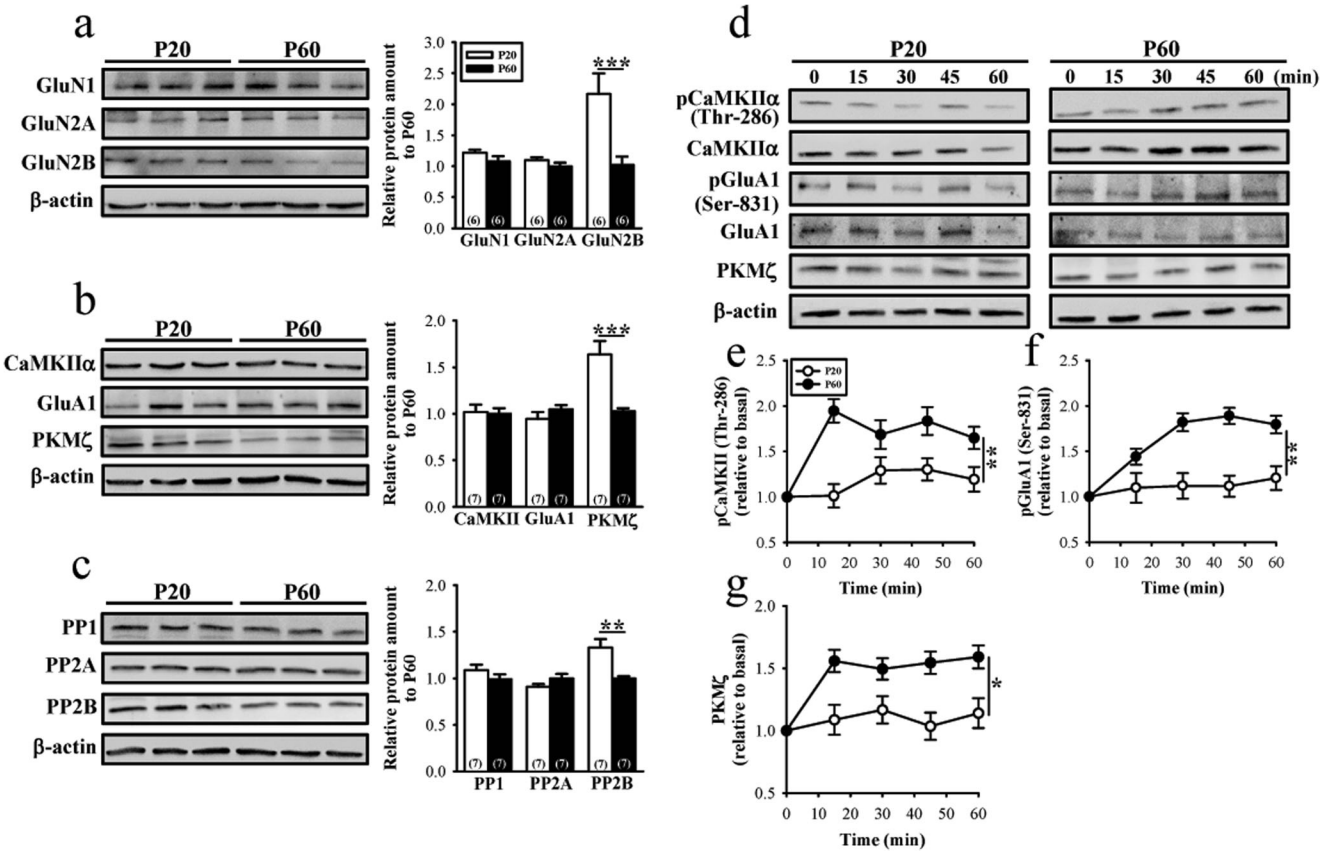

Fig. 4 P20 and P60 mice show differential expression of GluN2B, PKMζ, and PP2B signaling in hippocampal CA1 region. **a** Representative Western blot and summary bar graphs depicting protein levels of GluN1, GluN2A, and GluN2B in hippocampal CA1 tissue homogenates from P20 and P60 mice ($n = 6$ in each group). **b** Representative Western blot and summary bar graphs depicting protein levels of CaMKIIα, GluA1, and PKMζ in hippocampal CA1 tissue homogenates from P20 and P60 mice ($n = 7$ in each group). **c** Representative Western blot and summary bar graphs depicting protein levels of PP1, PP2A, and PP2B in hippocampal CA1 tissue homogenates from P20 and P60 mice ($n = 7$ in each group). **d–g** Representative Western blot and summary time course experiments showing comparisons of HFS (100 Hz, 1 s)-induced pCaMKIIα (Thr286) (**e**), pGluA1 (Ser831) (**f**), and PKMζ (**g**) expression in slices from P20 and P60 mice ($n = 8$ in each group). $^{*}p < 0.05$, $^{**}p < 0.01$, and $^{***}p < 0.001$ compared with P60 group. Error bars indicate SEM

Likewise, HFS also induced a significant increase in PKMζ levels in slices from P60 mice but this increase was not observed in slices from P20 mice ($F_{(4,70)} = 2.98$, $p < 0.05$; Fig. 4d, g).

Pharmacological Blockade of GluN2B-Containing NMDAR or PP2B Increases Memory Persistence in Infant Mice

We next explored whether decreasing GluN2B-containing NMDAR or PP2B activity before training could mitigate accelerated forgetting observed in infant mice. Therefore, the selective GluN2B-NMDAR inhibitor ifenprodil and the PP2B inhibitor cyclosporin A were used. We bilaterally infused ifenprodil (5 μg/μl) into the DH 15 min before OLM or CFC training (Fig. 5a). When long-term OLM was tested 24 h after training, there was no significant difference between P20 and P60 mice in the discrimination index ($t_{(16)} = 1.21$, $p = 0.24$; unpaired Student's t test; Fig. 5b). Likewise, P20 and P60 mice exhibited similar levels of freezing in the conditioning context when tested 24 h postconditioning ($t_{(14)} = 0.55$, $p = 0.59$; unpaired Student's t test; Fig. 5c). Similar results were also obtained in mice that received bilateral infusions of cyclosporin A (0.2 μg/μl) into the DH 15 min before OLM or CFC training. No significant difference between P20 and P60 mice was detected in the discrimination index when tested 24 h after OLM training ($t_{(17)} = 1.72$, $p = 0.11$; unpaired Student's t test; Fig. 5b). Twenty-four hours after CFC training, P20 and P60 mice exhibited comparable levels of freezing in the conditioning context ($t_{(14)} = 0.64$, $p = 0.53$; unpaired Student's t test; Fig. 5c).

Reducing GluN2B-Containing NMDAR or PP Activities Rescues E-LTP Deficit in Infant Mice

We finally examined whether decreasing GluN2B-containing NMDAR or PP2B activity might restore E-LTP deficit observed in infant mice. There was a significant difference between slices from P20 and P60 mice in the induction of E-LTP

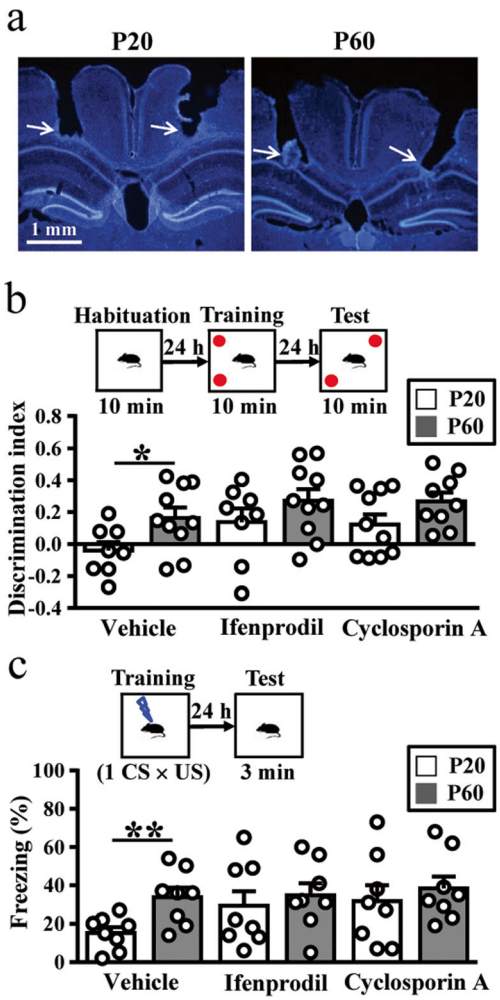

Fig. 5 Ifenprodil and cyclosporin A rescue the OLM and CFC performance in infant mice. **a** Representative coronal sections showing bilateral cannula tracks (arrow) targeting the dorsal hippocampus of P20 and P60 mice. **b** Schematic representations of the OLM task (upper panel). Summary bar graphs depicting the OLM performance in P20 and P60 mice treated with vehicle (DMSO, 10% in PBS), ifenprodil (5 μg/μl), or cyclosporin A (0.2 μg/μl) 15 min before OLM training. Data were obtained from 8 to 10 mice in each group. **c** Schematic representations of the training protocol for the CFC test (upper panel). Summary bar graphs depicting the 24 h delayed fear memory retention test in P20 and P60 mice treated with vehicle, ifenprodil (5 μg/μl) or cyclosporin A (0.2 μg/μl) 15 min before CFC training. Data were obtained from eight mice in each group. $*p < 0.05$ and $**p < 0.01$ compared with P60 group. Error bars indicate SEM

in the treatment with vehicle control (0.1% DMSO) ($p < 0.01$; Mann-Whitney *U* test; Fig. 6a, e). A single train of HFS produced comparable E-LTP in slices from P20 and P60 mice in the presence of ifenprodil (3 μM) ($p = 0.69$; Mann-Whitney *U* test; Fig. 6b, e). Likewise, cyclosporin A (250 μM) treatment significantly prevented E-LTP deficit in slices from P20 mice compared to those from P60 mice ($p = 0.62$; Mann-Whitney *U* test; Fig. 6c, e). Because PP2B can indirectly increase protein phosphatase 1 (PP1) activity by a mechanism to dephosphorylate the protein inhibitor-1 [30] and PP1 can act as an inhibitory constraint on E-LTP [31], we also determined whether blocking PP1 activity affects the induction of E-LTP in P20 mice. Treatment with okadaic acid (1 μM), an inhibitor of both PP1 and PP2A, significantly prevented E-LTP deficit in slices from P20 mice compared to those from P60 mice ($p = 0.80$; Mann-Whitney *U* test; Fig. 6d, e).

Discussion

It has been proposed that IA may simply result from the immaturity of the infant brain. According to this idea, the neural circuits and cellular mechanisms underlying memory formation are still underdeveloped and lack functional competence [4]. To our knowledge, this study provides the first demonstration that developmental immaturity of the maintenance mechanisms for LTP contributes the occurrence of IA. In support of this, we found that P20 mice display impaired hippocampal CA1 E-LTP and parallel deficits in hippocampus-dependent long-term memory retention compared to adult P60 mice. More importantly, we show that pharmacological blockade of GluN2B-containing NMDAR or PP2B activity restores E-LTP deficit and prolongs memory retention in P20 mice. Our results suggest that the expression profiles of molecules known to play critical roles in long-term synaptic plasticity are insufficiently mature during the IA period, which would interfere with long-term memory maintenance.

Based on the age of emergence of learning and cognitive functions, Madsen and Kim [1] proposed that rodents at P10-P12 are approaching the end of infancy (equivalent to one human year), at P12-P21 are in the juvenile period (one to seven human years), and at P28 are in adolescent period. While a series of studies by Frankland and his colleagues used P17 mice to determine the neurobiological bases of IA [10, 32], P20 mice were chosen in our current study. This is because mice at P13-P17 exhibited substantially spontaneous freezing to the conditioning context without receiving paired footshock training [32], which may influence the measures of conditioned fear response in the CFC test. We found that P20 mice are capable of remembering object locations where they have previously encountered after a short delay in the OLM task (Fig. 1a); however, these memories are not expressed over the long term (Fig. 1b). Similarly, P20 mice fear conditioned by a single conditioned stimulus (CS)-unconditioned stimulus (US) pairing paradigm shows impaired retention of contextual fear memory when tested 24 h later (Fig. 1d). Our findings that P20 mice received three CS-US pairings exhibit fear memory retention similar to that of P60 mice, suggesting that the ability to associate the context with the footshock is functionally competent at P20, consistent with previous reports [10, 32]. These observations echo the current concept that IA is not caused by insufficient learning during training [1, 8]. Moreover, the mechanisms that drive forgetting can be overcome by increasing training strength during the acquisition phase.

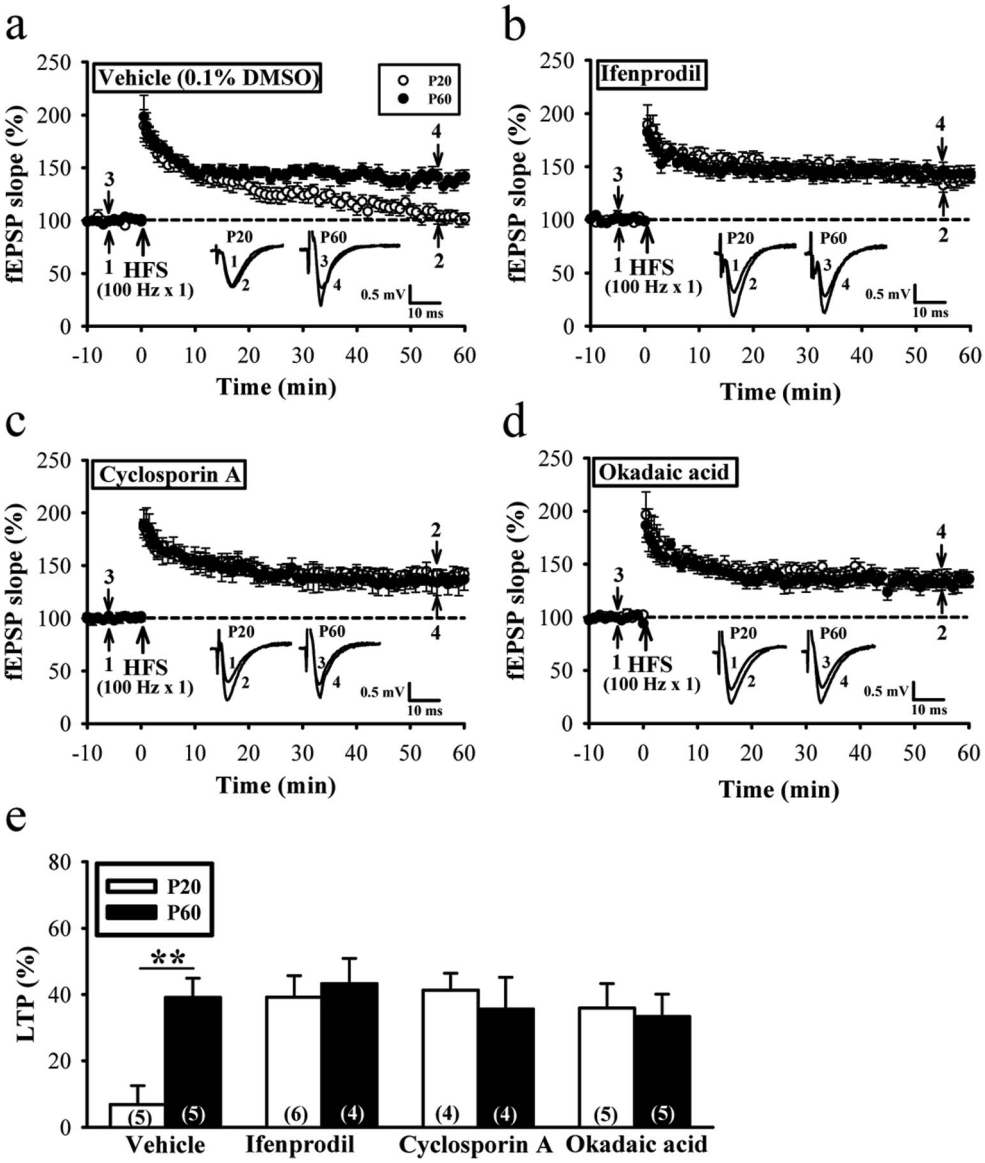

Fig. 6 Reducing GluN2B-containing NMDAR or PP activities rescues E-LTP deficit in P20 mice. **a** Summary of experiments showing the induction of E-LTP in slices from P20 and P60 mice in the presence of vehicle (0.1% DMSO). **b** Summary of experiments showing the induction of E-LTP in slices from P20 and P60 mice in the presence of ifenprodil (3 μM). **c** Summary of experiments showing the induction of E-LTP in slices from P20 and P60 mice in the presence of cyclosporin A (250 μM). **d** Summary of experiments showing the induction of E-LTP in slices from P20 and P60 mice in the presence of okadaic acid (1 μM). **e** Summary bar graphs comparing average magnitudes of E-LTP in slices from P20 and P60 mice with different treatment as indicated. The magnitudes of LTP were measured at 50–60 min after HFS. The total number of animals examined is indicated by *n* in parenthesis. $^{**}p < 0.01$ compared with P60 group. Error bars indicate SEM

LTP is widely considered to be one of the major mechanisms underlying memory storage [14, 15]. In the well-studied case of the Schaffer collateral-CA1 synapses, the induction of LTP requires activation of NMDARs that leads to a rise in the intracellular calcium, activation of CaMKII, and subsequent phosphorylation of the AMPAR subunits, resulting in an augmentation of their trafficking and function [17, 33, 34]. Moreover, the maintenance of LTP relies on increased synaptic insertion and stabilization of AMPARs [17, 35]. Our results show that E-LTP decays significantly faster in P20 than P60 mice, suggesting that molecular mechanisms responsible for the maintenance of E-LTP are insufficiently mature at P20. Indeed, in slices from P20 mice, a single train of HFS we used to induce E-LTP was insufficient to trigger a sustained rise in CaMKII activity and AMPAR phosphorylation at GluA1 Ser831 (Fig. 4d–f), which are crucial for maintaining E-LTP [36]. As the level of GluA1 phosphorylation at Ser831 is regulated by a balance between CaMKII and PP1 activity [22, 36], it is possible that the lower level of HFS-triggered GluA1 Ser831 in P20 mice is associated with a higher endogenous PP2B expression (Fig. 4c), which promotes PP1 activity indirectly through reduced phosphorylation of protein inhibitor-1 [30]. In addition to CaMKII and PP1, another candidate protein involved in the maintenance of LTP is PKMζ. While the role of PKMζ in LTP maintenance remains inconclusive [37–39], it is clear that the LTP-inducing HFS triggered significant increases in PKMζ protein expression in hippocampal CA1 region. However, we found that this increase is restricted in P60 mice (Fig. 4g), while P20 mice express higher basal level of PKMζ protein than P60 mice (Fig. 4b). One possible explanation for this finding is that high PKMζ expression may alter the prolyl-peptidyl isomerase

Pin1 phosphorylation and activity [40], making less additional PKMζ protein synthesis following LTP induction [41].

A hallmark feature of NMDARs is the early postnatal developmental switch in subunit composition from predominantly GluN2B- to GluN2A-containing receptors [42, 43]. Differences in subunit composition of NMDARs can confer distinct biophysical properties and couple to different downstream signaling cascades [43]. Consistently, we observed that GluN2B protein abundance is high at P20 and declines by P60, whereas GluN1 and GluN2A protein levels are not different between groups (Fig. 4a). Our finding that GluN2B-specific antagonist ifenprodil successfully restored E-LTP deficit supports the notion that the impaired E-LTP maintenance in P20 mice is likely a result of excess GluN2B-containing NMDAR activation. Our findings are in line with previous work, demonstrating that E-LTP decay is associated with activation of GluN2B-containing NMDARs [44, 45]. While the mechanism by which NMDAR activation mediates LTP decay remains to be elucidated, an active process that promotes AMPAR removal from synapses could be involved. In this context, it has recently been shown that inhibition of AMPAR endocytosis can prolong the duration of LTP [46]. Moreover, consistent with previous findings [29], we observed that P20 mice exhibit smaller synaptic responses than P60 mice. Because this reduction is reliably associated with an increase in PPF ratio and a decrease in mEPSC frequency, we speculate that developmental difference in basal synaptic transmission is majorly presynaptic in origin. Given that the input-output curve difference between P20 and P60 mice was not rescued by ifenprodil or cyclosporin A treatments (data not shown), this difference is not caused by the excess GluN2B-containing NMDAR activation or PP2B activity in hippocampal CA1 region.

Like memory formation, LTP can be divided into at least two temporally distinct phases that are fundamentally different in their induction protocols and biochemical features [47, 48]. A surprising result was that only E-LTP induced by a single HFS train, but not L-LTP, is impaired in P20 mice, suggesting that repeated HFS is sufficient to overcome the factors linked to impaired E-LTP maintenance in P20 mice and that L-LTP is not only a composite of gradually decaying E-LTP. In parallel, we found that P20 and P60 mice exhibited similar levels of freezing behavior when exposed to a more intense training paradigm (Fig. 1e). In most studies of IA, memory retention deficits are typically observed 7 days or even longer after multiple training trials [10, 49]. We extend these findings by demonstrating that forgetting can occur as early as 1 day after training in infant mice that received a weak training protocol. This is in line with a recent report showing that memory for inhibitory avoidance training in infant rats completely decays by 1 day later [8]. In the adult brain, forgetting of long-term memory specifically requires activation of GluN2B-containing NMDAR and PP2B [44, 50]. Our results confirm these findings, as systemic injections of ifenprodil and cyclosporin A mitigated forgetting in P20 mice. This might suggest that infant and adult mice share similar neurobiological mechanisms underpinning the time-dependent forgetting of long-term memories and that the high level activity of PP2B mediates accelerated forgetting in infant mice. These findings strongly imply that pharmacologic blockade of GluN2B-containing NMDAR and PP2B is able to enhance memory persistence. Further studies are required to validate the translational application of these findings to the treatment of memory and cognitive disorders. Whereas thus far our data show that accelerated forgetting during infancy seems to be related to storage failure or accelerated decay, we could not exclude the possibility that forgetting may also result from a failure in memory retrieval. In fact, reminder training has been shown to effectively reinstate memory acquired during the IA period [2, 8]. Since recent engram labelling technology allows subsequent manipulation of components of specific memory engrams in particular brain regions [51, 52], in light of the role of retrieval deficit, it would be interesting to explore whether reactivating engram cells and their associated circuits could successfully recall infant memories in future studies.

Interestingly, our data demonstrate no significant differences between P20 and P60 mice in short-term recall of OLM and CFC memories. These findings do not contradict the observation that P20 mice exhibit a significantly faster decay of E-LTP compared to P60 mice. Considering that LTP has generally been proposed to participate in memory consolidation processes that involve transferring new learning from short-term to long-term memory storage, LTP expression could be dissociated from short-term memory. Indeed, there is abundant evidence for the existence of dissociation between the impaired E-LTP and intact short-term memory [53–55].

In conclusion, we provide compelling evidence that the remembering ability increases with development and maturation and suggest that the faster rate of forgetting at the infancy stage of development is due to the immaturity of the maintenance mechanisms for LTP. By using biochemical and pharmacological approaches, we show that excess forgetting-related GluN2B-containing NMDAR and PP2B activation in the hippocampus are associated with memory failures that occur during infancy. Our findings contribute a better understanding neurobiological mechanisms underlying IA and provide novel pharmacological strategies to reduce rate of forgetting.

Acknowledgements We thank the technical services provided by the Bio-image Core Facility of the National Core Facility Program for Biotechnology, Ministry of Science and Technology, Taiwan.

Funding Information This work was supported by research grants from the Ministry of Science and Technology (MOST 106-2320-B-006-026-MY3) and the National Health Research Institute (NHRI-EX106-10613NI and NHRI-EX107-10713NI), Taiwan.

Compliance with Ethical Standards

All experimental procedures complied with the National Institutes of Health Guide for the Care and Use of Laboratory Animals and were approved by the Institutional Animal Care and Use Committee of National Cheng Kung University.

Conflict of Interest The authors declare that they have no conflict of interest.

References

1. Madsen HB, Kim JH (2016) Ontogeny of memory: an update on 40 years of work on infantile amnesia. Behav Brain Res 298:4–14
2. Campbell BA, Spear NE (1972) Ontogeny of memory. Psychol Rev 79:215–236
3. Callaghan BL, Li S, Richardson R (2013) The elusive engram: what can infantile amnesia tell us about memory? Trends Neurosci 37: 47–53
4. Josselyn SA, Frankland PW (2012) Infantile amnesia: a neurogenic hypothesis. Learn Mem 19:423–433
5. Rovee-Collier CK, Gekoski MJ (1979) The economics of infancy: a review of conjugate reinforcement. Adv Child Dev Behav 13:195–255
6. Miller JS, Jagielo JA, Spear NE (1991) Differential effectiveness of various prior-cuing treatments in the reactivation and maintenance of memory. J Exp Psychol Anim Behav Process 17:249–258
7. Kim JH, Richardson R (2007) Immediate post-reminder injection of GABA agonist midazolam attenuates reactivation of forgotten fear in the infant rat. Behav Neurosci 121:1328–1332
8. Travaglia A, Bisaz R, Sweet ES, Blitzer RD, Alberini CM (2016) Infantile amnesia reflects a developmental critical period for hippocampal learning. Nat Neurosci 19:1225–1233
9. Frankland PW, Köhler S, Josselyn SA (2013) Hippocampal neurogenesis and forgetting. Trends Neurosci 36:497–503
10. Akers KG, Martinez-Canabal A, Restivo L, Yiu AP, De Cristofaro A, Hsiang HL, Wheeler AL, Guskjolen A et al (2014) Hippocampal neurogenesis regulates forgetting during adulthood and infancy. Science 344:598–602
11. Kandel ER, Dudai Y, Mayford MR (2014) The molecular and systems biology of memory. Cell 157:163–186
12. Poo MM, Pignatelli M, Ryan TJ, Tonegawa S, Bonhoeffer T, Martin KC, Rudenko A, Tsai LH et al (2016) What is memory? The present state of the engram. BMC Biol 14:40
13. Nicoll RA, Roche KW (2013) Long-term potentiation: peeling the onion. Neuropharmacology 74:18–22
14. Cooke SF, Bliss TV (2006) Plasticity in the human central nervous system. Brain 129:1659–1673
15. Mayford M, Siegelbaum SA, Kandel ER (2012) Synapses and memory storage. Cold Spring Harb Perspect Biol 4:a005751
16. Winder DG, Sweatt JD (2001) Roles of serine/threonine phosphatases in hippocampal synaptic plasticity. Nat Rev Neurosci 2:461–474
17. Malenka RC, Bear MF (2004) LTP and LTD: an embarrassment of riches. Neuron 44:5–21
18. Yasuda H, Barth AL, Stellwagen D, Malenka RC (2003) A developmental switch in the signaling cascades for LTP induction. Nat Neurosci 6:15–16
19. Huang CC, Chou PH, Yang CH, Hsu KS (2005) Neonatal isolation accelerates the developmental switch in the signalling cascades for long-term potentiation induction. J Physiol 569:789–799
20. Yang CH, Huang CC, Hsu KS (2012) A critical role for protein tyrosine phosphatase nonreceptor type 5 in determining individual susceptibility to develop stress-related cognitive and morphological changes. J Neurosci 32:7550–7562
21. Huang YF, Yang CH, Huang CC, Tai MH, Hsu KS (2010) Pharmacological and genetic accumulation of hypoxia-inducible factor-1alpha enhances excitatory synaptic transmission in hippocampal neurons through the production of vascular endothelial growth factor. J Neurosci 30:6080–6093
22. Huang CC, Liang YC, Hsu KS (2001) Characterization of the mechanism underlying the reversal of long term potentiation by low frequency stimulation at hippocampal CA1 synapses. J Biol Chem 276:48108–48117
23. Valverde F (1998) Golgi atlas of the postnatal mouse brain, 15th edn. Springer-Verlag, Chicago
24. Franklin K, Paxinos G (2008) The mouse brain in stereotaxic coordinates, 3rd edn. Elsevier Academic Press, San Diego
25. Kojima N, Sakamoto T, Endo S, Niki H (2005) Impairment of conditioned freezing to tone, but not to context, in Fyn-transgenic mice: relationship to NMDA receptor subunit 2B function. Eur J Neurosci 21:1359–1369
26. Mouri A, Noda Y, Shimizu S, Tsujimoto Y, Nabeshima T (2010) The role of cyclophilin D in learning and memory. Hippocampus 20:293–304
27. Izquierdo LA, Barros DM, Vianna MR, Coitinho A, deDavid e Silva T, Choi H, Moletta B, Medina JH et al (2002) Molecular pharmacological dissection of short- and long-term memory. Cell Mol Neurobiol 22:269–287
28. Han JH, Kushner SA, Yiu AP, Cole CJ, Matynia A, Brown RA, Neve RL, Guzowski JF et al (2007) Neuronal competition and selection during memory formation. Science 316:457–460
29. Hussain RJ, Carpenter DO (2001) Development of synaptic responses and plasticity at the SC-CA1 and MF-CA3 synapses in rat hippocampus. Cell Mol Neurobiol 21:357–368
30. Shenolikar S, Nairn AC (1991) Protein phosphatases: recent progress. Adv Second Messenger Phosphoprotein Res 23:1–121
31. Blitzer RD, Connor JH, Brown GP, Wong T, Shenolikar S, Iyengar R, Landau EM (1998) Gating of CaMKII by cAMP-regulated protein phosphatase activity during LTP. Science 280:1940–1942
32. Akers KG, Arruda-Carvalho M, Josselyn SA, Frankland PW (2012) Ontogeny of contextual fear memory formation, specificity, and persistence in mice. Learn Mem 19:598–604
33. Lisman J, Yasuda R, Raghavachari S (2012) Mechanisms of CaMKII action in long-term potentiation. Nat Rev Neurosci 13: 169–182
34. Herring BE, Nicoll RA (2016) Long-term potentiation: from CaMKII to AMPA receptor trafficking. Annu Rev Physiol 78: 351–365
35. Anggono V, Huganir RL (2012) Regulation of AMPA receptor trafficking and synaptic plasticity. Curr Opin Neurobiol 22:461–469
36. Lee HK, Barbarosie M, Kameyama K, Bear MF, Huganir RL (2000) Regulation of distinct AMPA receptor phosphorylation sites during bidirectional synaptic plasticity. Nature 405:955–959
37. Ling DS, Benardo LS, Serrano PA, Blace N, Kelly MT, Crary JF, Sacktor TC (2002) Protein kinase Mζ is necessary and sufficient for LTP maintenance. Nat Neurosci 5:295–296
38. Sacktor TC (2011) How does PKMζ maintain long-term memory? Nat Rev Neurosci 12:9–15
39. Volk LJ, Bachman JL, Johnson R, Yu Y, Huganir RL (2013) PKMζ is not required for hippocampal synaptic plasticity, learning and memory. Nature 493:420–423
40. Westmark PR, Westmark CJ, Wang S, Levenson J, O'Riordan KJ, Burger C, Malter JS (2010) Pin1 and PKMζ sequentially control dendritic protein synthesis. Sci Signal 3:ra18
41. Schuette SR, Fernández-Fernández D, Lamla T, Rosenbrock H, Hobson S (2016) Overexpression of protein kinase Mζ in the hippocampus enhances long-term potentiation and long-term contextual but not cued fear memory in rats. J Neurosci 36:4313–4324

42. Yashiro K, Philpot BD (2008) Regulation of NMDA receptor subunit expression and its implications for LTD, LTP, and metaplasticity. Neuropharmacology 55:1081–1094
43. Paoletti P, Bellone C, Zhou Q (2013) NMDA receptor subunit diversity: impact on receptor properties, synaptic plasticity and disease. Nat Rev Neurosci 14:383–400
44. Sachser RM, Santana F, Crestani AP, Lunardi P, Pedraza LK, Quillfeldt JA, Hardt O, Alvares Lde O (2016) Forgetting of long-term memory requires activation of NMDA receptors, L-type voltage-dependent Ca^{2+} channels, and calcineurin. Sci Rep 6:22771
45. Wang YT, Huang CC, Lin YS, Huang WF, Yang CY, Lee CC, Yeh CM, Hsu KS (2017) Conditional deletion of Eps8 reduces hippocampal synaptic plasticity and impairs cognitive function. Neuropharmacology 112:113–123
46. Dong Z, Han H, Li H, Bai Y, Wang W, Tu M, Peng Y, Zhou L et al (2015) Long-term potentiation decay and memory loss are mediated by AMPAR endocytosis. J Clin Invest 125:234–247
47. Frey U, Huang YY, Kandel ER (1993) Effects of cAMP simulate a late stage of LTP in hippocampal CA1 neurons. Science 260:1661–1664
48. Kelleher RJ 3rd, Govindarajan A, Tonegawa S (2004) Translational regulatory mechanisms in persistent forms of synaptic plasticity. Neuron 44:59–73
49. Cowan CS, Callaghan BL, Richardson R (2016) The effects of a probiotic formulation (*Lactobacillus rhamnosus* and *L. helveticus*) on developmental trajectories of emotional learning in stressed infant rats. Transl Psychiatry 6:e823
50. Shinohara K, Hata T (2014) Post-acquisition hippocampal NMDA receptor blockade sustains retention of spatial reference memory in Morris water maze. Behav Brain Res 259:261–267
51. Liu X, Ramirez S, Pang PT, Puryear CB, Govindarajan A, Deisseroth K, Tonegawa S (2012) Optogenetic stimulation of a hippocampal engram activates fear memory recall. Nature 484: 381–385
52. Tanaka KZ, Pevzner A, Hamidi AB, Nakazawa Y, Graham J, Wiltgen BJ (2014) Cortical representations are reinstated by the hippocampus during memory retrieval. Neuron 84:347–354
53. Lu YM, Jia Z, Janus C, Henderson JT, Gerlai R, Wojtowicz JM, Roder JC (1997) Mice lacking metabotropic glutamate receptor 5 show impaired learning and reduced CA1 long-term potentiation (LTP) but normal CA3 LTP. J Neurosci 17:5196–5205
54. Thiels E, Urban NN, Gonzalez-Burgos GR, Kanterewicz BI, Barrionuevo G, Chu CT, Oury TD, Klann E (2000) Impairment of long-term potentiation and associative memory in mice that overexpress extracellular superoxide dismutase. J Neurosci 20: 7631–7639
55. Plath N, Ohana O, Dammermann B, Errington ML, Schmitz D, Gross C, Mao X, Engelsberg A et al (2006) Arc/Arg3.1 is essential for the consolidation of synaptic plasticity and memories. Neuron 52:437–444